The Clay Minerals Society Workshop Lectures Series, Vol. 21 (2016), Chapter 17, 219–229

THE INTERNAL ARCHITECTURE AND PERMEABILITY STRUCTURES OF FAULTS IN SHALE FORMATIONS

Pierre Dick[1,*], Charles Wittebroodt[1], Christelle Courbet[1], Juuso Sammaljärvi[2], Imène Estève[3], Jean-Michel Matray[1], Marja Siitari-Kauppi[2], Miko Voutilainen[2], and Alexandre Dauzères[1]

[1]*IRSN-Institut de Radioprotection et de Sûreté Nucléaire, BP 17, F-92262 Fontenay-aux-Roses, France*
[2]*Laboratory of Radiochemistry, Department of Chemistry, FI-00014 University of Helsinki, Finland*
[3]*Institut de Minéralogie et de Physique des Milieux Condensés (IMPMC), UMR 7590 CNRS-UPMC/Paris VI-IRD, Case 115, 4 place Jussieu, 75252 Paris Cedex 05, France*
[*]*e-mail: pierre.dick@irsn.fr*

The evaluation of fluid flow through fractures and faults is of primary importance for the long-term performance assessment of radioactive waste repositories in shale formations and could be used to assess CO_2 storage security or the integrity of caprocks and reservoir capacity. This study focuses on the structural evolution within brittle to ductile shear zone in order to understand permeability enhancement and sealing processes affecting a strike-slip fault system within the Toarcian shale formation from the Tournemire Underground Research Laboratory (URL), southern France. A combination of quantitative field measurements and laboratory and *in situ* experiments was used to estimate the fluid-flow properties of a fractured shale formation. Results indicate that microfractures govern the matrix porosity in the damage zone and play an increasingly dominant role in fluid flow along the boundary between fault core and fault damage zone.

1. Introduction

Gas and solute will always follow the channel of least resistance in their flow through low-permeability formations. When such media are transected by permeable faults or interconnected fractures, cross-formational flow could occur along these discontinuities (Lalieux and Horseman, 1996). Assessing the amount of fluid flow through faults and fractures is, therefore, one of the main priorities for the performance assessment for a Deep Geological Repository (DGR) located in clay formations. Nevertheless, the hydraulic properties of such faults and fractures still remain difficult to predict due to their heterogeneous internal architecture. Bulk flow rates through or along fault zones are dependent on a number of factors including permeability variations, structural anisotropy, pressure differentials, and fluid viscosity (Caine *et al.,* 1996; Evans *et al.,* 1997; Cox, 1999; Wibberley *et al.,* 2008; Faulkner *et al.,* 2010; Seebeck *et al.,* 2014).

DOI: 10.1346/CMS-WLS-21.17

Moreover, measuring flow properties of fault zones is still subject to caution owing to the rare *in situ* flow data available which can be related directly to the structure of fault zones and surrounding rock volume (Evans *et al.,* 1997; Wibberley *et al.,* 2008; Faulkner *et al.,* 2010; Seebeck *et al.,* 2014).

In the present study, mapping of a fault-zone structure and *in situ* hydraulic tests within small-scale strike slip faulting affecting the low-permeability Tournemire shale formation in the Tournemire Underground Research Laboratory (URL) were combined.

The Tournemire URL has been developed by the French Institute for Radiological Protection and Nuclear Safety (IRSN) in order to ensure an independent assessment of the French National Radioactive Waste Management Agency's (ANDRA) Cigeo project (industrial geological disposal centre). Located on the western border of the Mesozoic sedimentary Causses Basin (SW France), the Tournemire URL crosses a thick Toarcian shale formation (~250 m) and is interbedded between two aquiferous limestone units. In addition to the 250 m thick overlying limestones, the hydrogeological characteristics of this site exhibit similarities with those measured by ANDRA in the Callovo-Oxfordian argillaceous formation at the Bure URL (Meuse/Haute Marne, France).

One of the objectives of IRSN's research programs is to evaluate the driving processes controlling water flux, and thus radionuclide migration, through an argillaceous formation. Because such rocks display very small values for both hydraulic conductivity (K_h) and water content (θ_e) (Matray *et al.,* 2007), diffusion is considered to be the main transport mechanism governing radionuclide migration. The occurrence of natural fractures in such formations allows increasing water flux and thus radionuclide migration, however (Savoye *et al.,* 2003).

Fluid circulations along the strike-slip fault zones at the Tournemire URL occurred principally during the two Pyrenean compressive tectonic events that affected the Causses basin (Constantin *et al.,* 2004; Lefevre *et al.,* 2014). The first tectonic phase enabled fluid flow along pre-existing bedding and brecciated shear zones, whereas the second phase is only associated with shearing within the fault core (Lefevre *et al.,* 2015). The microstructural study of these faults indicate that they were alternately and temporarily impermeable, permeable, or semi-permeable during the tectonic activity (Constantin *et al.,* 2004). These hydraulic states were controlled by the nature and the architecture of the microstructures and by variations in the petrophysical properties of the rock in the fault core and damage zone of the faults (Constantin *et al.,* 2004).

Accurate detection of such faults in clayey rocks from surface geophysical surveys and from existing underground drifts remains a major challenge, even using high-resolution seismic surveys. For this reason, IRSN carried out a 3D high-resolution seismic survey 250 m above the Tournemire URL on the Larzac plateau in an attempt to detect the fault zones described above (Cabrera, 2002). This survey covered an area of 1.5 km^2 with 846 shot points and around 900 receive points. The trace spacing was 10 m, with frequencies ranging from 40 to 140 Hz, while the vertical resolution was a few meters. Due to the shale's weak seismic impedance contrast and the small vertical offset, the fault zone could not be identified in the shale formation. The subvertical fault was successfully picked out by the seismic data in the limestone layer underlying the shale formation, as well as at the interface between these two

layers, however. Furthermore, because of the poor spatial coverage of seismic data in the upper limestone, the poor signal-to-noise ratio of the seismic data at shallow depths, and the presence of karsts in the upper limestone layer, the fault zone was not detected in the upper limestone formation.

Considering that such structures might be overlooked during the site characterization of a DGR, an evaluation of fluid flow through these faults and fractures appears important for the DGR safety assessment. Consequently, IRSN has designed a series of *in situ* and laboratory experiments to evaluate permeability-porosity evolution through a clay-rich fault zone and in an undisturbed shale formation.

2. Materials and methods

The Tournemire URL is crossed by two main fault zones (F1 and F2) separated by a relatively undisturbed protolith (Bretaudeau *et al.,* 2014). The internal architecture and the geometry of the fault zones were determined by small-scale mapping of the galleries' walls and floor and through the geological and geophysical logging of >25 boreholes (Figure 1). F1 and F2 have a similar dip and dip-direction varying spatially between N170°-to-N010° and 60°-to-80°W (Lefevre *et al.,* 2015) and are characterized by reverse left-lateral strike slip movement (Peyaud *et al.,* 2006). The F1 fault zone exhibits a complex array of anastomosed fault surfaces consisting of brittle fractures and ductile shear bands, whereas F2 presents two main architectural elements: a central fault core which accommodates most of the displacement and a surrounding fault damage zone. The F2 fault core is 1 to 2 m thick and consists of thin dark bands of centimeter thick gouge, cataclastic and brecciated rock, as well as subvertical schistosity planes, folds and also lenses of less deformed rock (Figure 2). The damage zone is $4-5$ m wide in the hangingwall and $2-3$ m wide within the footwall. The damage zones, if formed by a dense network of small faults, fractures, and veins, were completely sealed by crystalline calcite. Bedding planes in the damage zone and undisturbed protolith dip gently towards the North ($5-10°$). However, a gradual increase in bedding plane dip can be seen towards the fault core. The boundary between the protolith and the damage zone is diffuse, whereas the boundary between the fault core and damage zone is sharp and is lined by a thin band of gouge. A dolomitic horizon marker crossed by several boreholes on either side of the fault suggests that the amount of slip perpendicular to strike is $\sim 4-6$ m while slip along strike is estimated to be between 15 and 30 m (Figure 2).

Rock samples were collected from the fault zone and from the undisturbed rock through a 50 m long horizontal borehole (FR1). Geological mapping and borehole logging methods (optical borehole imaging, resistivity, spectral gamma-ray, and magnetic susceptibility) enabled the accurate localization of the fault zone, the selection of representative shale samples (undisturbed and fractured), and the performance of mineralogical and petrophysical characterizations.

To understand the background of mineral assemblages and the average clay contents of the shale formation, 15 powdered samples, extracted from the undisturbed, damage,

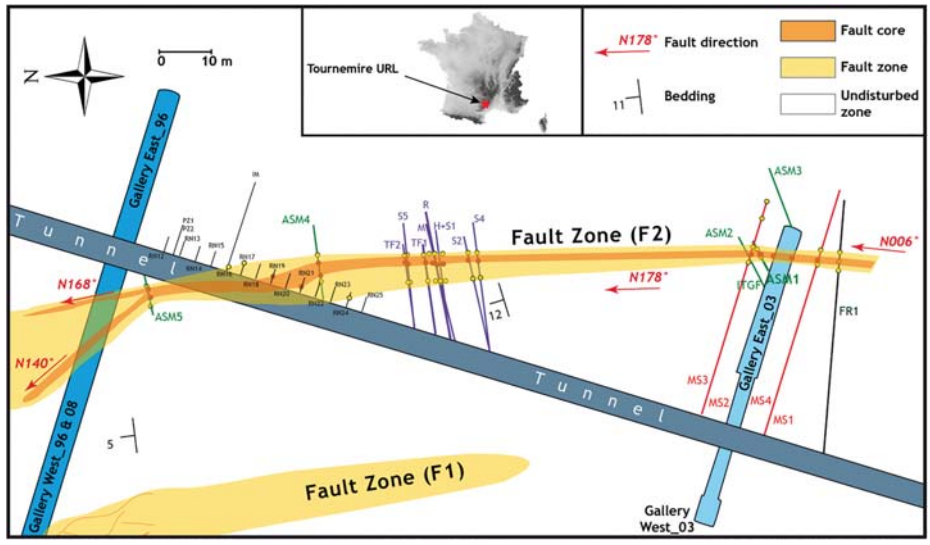

Figure 1. Simplified map of the Tournemire Underground Research Laboratory (URL). The spatial distribution of the fault zones was determined from borehole logging and geological mapping from the galleries' floor, walls, and roof. The three main components of the fault zones are: the fault core, the damage zone, and the undisturbed protolith. The fault core corresponds to the area of the fault zone where the majority of the displacement has taken place and includes gouge, cataclasite, kink bands, and subvertical schistosity. The damage zone forms an intermediate zone from the fault core to the protolith. The damage zone includes small faults, brittle fractures, and veins. The protolith represents the undeformed or non-fractured rock. The boundary between the protolith and damage zone is gradual while the boundary between the damage zone and fault core is sharp.

and fault core zones, were examined by X-ray diffraction (XRD) analysis. To identify and quantify clay minerals of clay-size fraction, glass slides of oriented samples were made. All samples were disaggregated in distilled water and after centrifugation, draft suspensions of <2 μm were deposited on glass slides. Further, ethylene glycol was used to hydrate the clay samples so as to recognize swelling clays (illite-smectite interstratifications). In addition, six samples (two from the fault core and four from undisturbed shale) were analyzed to determine both specific surface area values based on the BET equation (Brunauer *et al.,* 1938), and pore-size distribution calculated by the Barrett-Joyner-Hallenda (BJH) method (Barrett *et al.,* 1951).

Immediately after drilling operations, a Modular Multi-Packer System (MMPS) was installed in the borehole for hydraulic testing (pulse-test) within the fault zone and adjacent, undisturbed rock. This device allows up to three individual packer modules with a diameter of 101 mm to be coupled in a variety of configurations. Each packer module consists of a stand-alone unit with a packer inflation line and both flow- and pressure-measurement lines. Packer pressures are controlled by a manometer installed in the control unit, while both a manometer and a pressure transducer control interval pressures. The chosen configuration consists of two 20-cm intervals (P1 & P3) and one 3-m interval (P2); each interval is sealed by 150-cm long packers. The P1 and P3

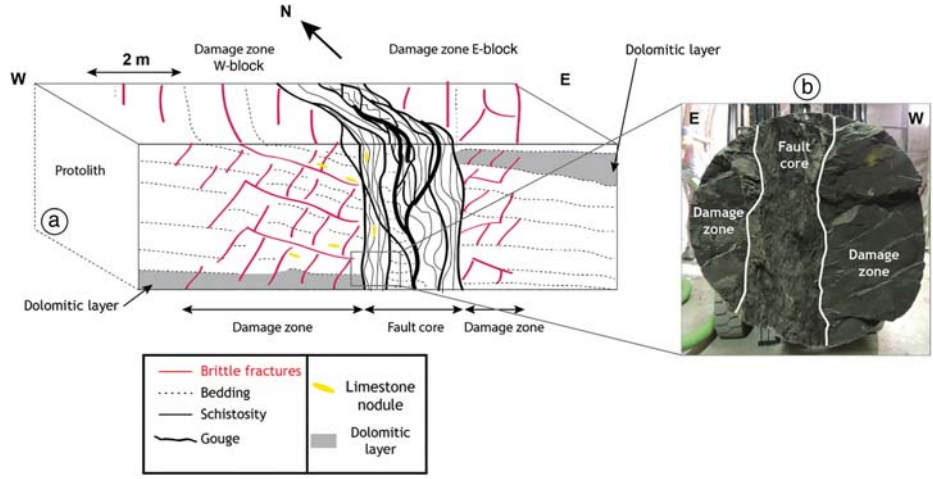

Figure 2. (a) Conceptual model of the Tournemire fault zone. The fault core is characterized by subparallel anastomosing gouge bands that isolate lenses of undeformed rock or brittle-to-ductile structures such as subvertical schistosity, folds, fractures, and veins. The damage zone is characterized by low-dipping brittle structures (fractures and veins) and sub-horizontal bedding. The protolith presents large-scale regional deformation and no fractures. (b) 400 mm diameter core sample extracted from the fault. The core shows the heterogeneous deformation patterns within the fault, *e.g.* lenses of highly strained shear zones surrounded by less strained rocks (damage zone structures).

intervals are located in the undisturbed footwall and hangingwall blocks, respectively, whereas the P2 interval is centered within the fault zone in order to measure the hydraulic conductivity of the fault core and the adjacent damage zones. All test intervals were saturated with water from the upper aquifer, the composition of which is close to that of interstitial shale waters to avoid any osmotic and chemical effects. Pulse tests were carried out immediately after initial pressure recovery by an injection of a known water volume. Injection pressures of 1 bar were instantly generated with a hand pump.

The total porosity of the rock was determined using a multi-scale approach; (1) by volumetric and gravimetric methods for bulk properties; (2) Broad Ion Beam (BIB)/ Focused Ion Beam (FIB)-Scanning Electron Microscopy (SEM) techniques for macro-porosity investigations; and (3) autoradiography methods using the C-14-PMMA impregnation technique (Sammaljärvi *et al.,* 2012) developed to investigate the meso- to nano-porosity and pore structure in the rock matrix.

3. Results and discussion

3.1. Fault architecture

The studied fault zone is characterized by two major components: a damage zone and a fault core (Figure 2). The fault core consists of a heterogeneous brittle to cataclastic zone where localized slip occurred principally along a thin (0.5–2 cm thick), fine-grained

black gouge. Throughout the fault plane, the total thickness of the fault core varies between 0 to 1.5 m. The damage zones include brittle fault-related deformation structures such as small faults, veins, fractures, and cleavage as well as sub-millimetric clay smears along brittle deformation bands. Strain inferred from anisotropy of magnetic susceptibility measurements indicate heterogeneous structural fabrics within the fault core, whereas the damage zone exhibits a progressive increase in deformation fabrics from its distal to internal domain (Dick *et al.,* 2013).

3.2. Porosity

Petrophysical results (Figure 3) indicate that the damage zone domain closest to the fault core and with the greatest abundance of deformation features also exhibits the largest porosity values (15–20%). In contrast, the smallest porosity values (~10%) were detected in the less deformed damage zone at greater distance from the fault core. Furthermore, due to localized grain crushing and fluid flow in shear bands within the fault core, the slip zone gouges can locally exhibit extremely low porosity values (<4%).

The preliminary results of the two imaging techniques used (BIB/FIB/SEM and autoradiography) display different trends. On the one hand, porosity values determined by autoradiography (Figure 4) for the undisturbed shale are consistent with those measured by petrophysical methods (~11%). On the other hand, results obtained from BIB-FIB-SEM (Figure 5) methods lead to smaller porosity values (1%) and lower pore interconnectivity, which is inconsistent with properties of Upper Toarcian

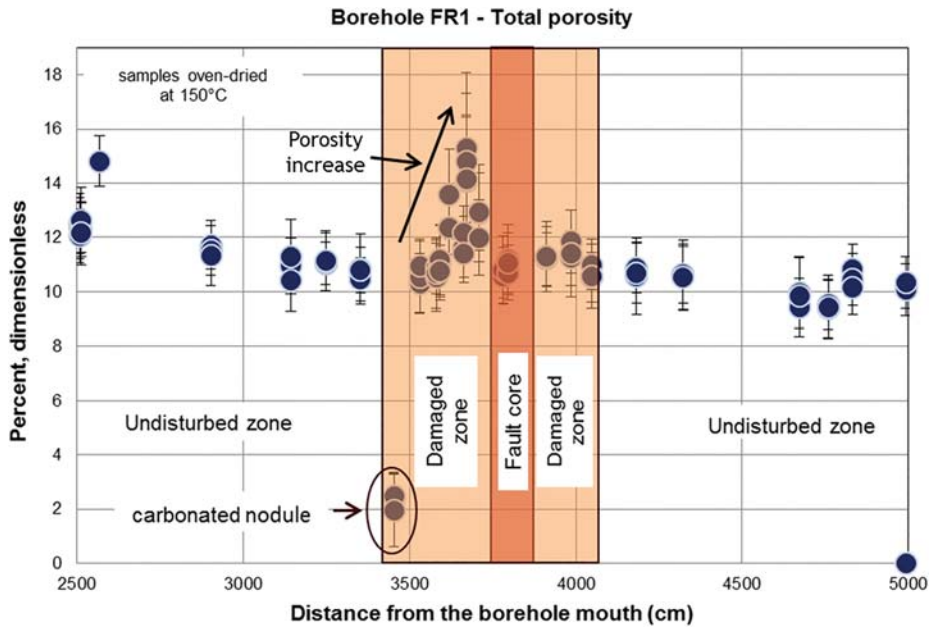

Figure 3. Bulk-sample porosity obtained from gravimetric methods.

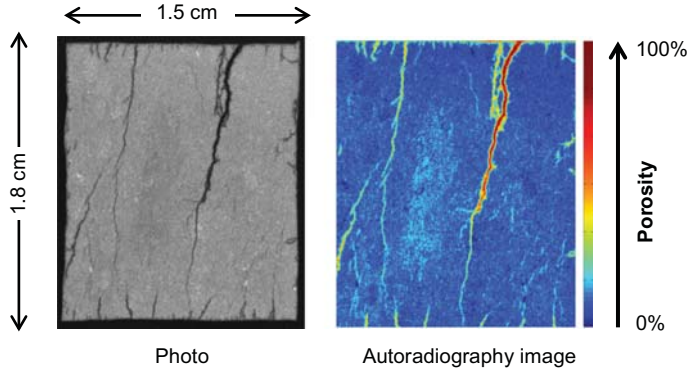

Figure 4. Spatial-porosity distribution based on quantitative autoradiography of an undisturbed sample impregnated with ^{14}C polymethylmethacrylate (PMMA). Fractures in the sample were due to the preparation method. Porosity values in the non-fractured zones (11%) are comparable with those obtained from bulk gravimetric methods, however.

argillaceous rock generally proposed in the literature (Altinier *et al.,* 2007; Bensenouci *et al.,* 2011). Such discrepancies may result from the different pore sizes investigated within these different methods. Indeed, the autoradiography method takes into account a larger part of the shale's pore network (diameter $\geq$ 4 nm) than does BIB-FIB-SEM (diameter $\geq$ 10 nm) and, thus, is more efficient at characterizing the variability in the shale's microspatial porosity.

The results show that shale samples taken from the fault zone are characterized by specific surface area values ranging from 21.68 $m^2 \cdot g^{-1}$ to 22.84 $m^2 \cdot g^{-1}$. These values are close to the mean specific surface area determined for the undisturbed rock samples (24.08 $m^2 \cdot g^{-1}$) which is in good agreement with literature data (Savoye *et al.,* 2001). The results also show that both undisturbed and fault-zone shale samples are characterized by a pore network comprising 30% of micro-pores (diameter

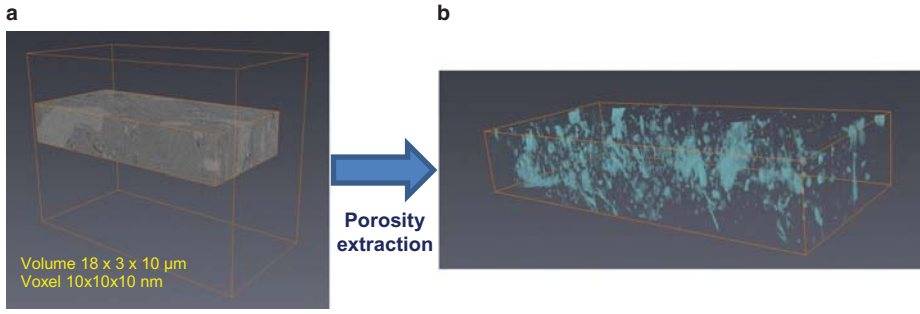

Figure 5. Three-dimensional reconstructed pore model from the undisturbed Tournemire shale from FIB-SEM imaging: (a) 1000 slices of SEM images are aligned and stacked; (b) three-dimensional stack converted to binary image of 0 and 1 voxel values are extracted to perform porosimetry analysis.

$<$10 nm). Moreover, 70% of this micro-porosity consists of pores with a diameter of $<$6 nm. For the petrophysical measurement results, specific surface area and pore size distribution values don't show large discrepancies between undisturbed rock samples and shale samples taken from the fault zone. Such results indicate that the fault zone also contains undisturbed shale blocks in addition to the fractured rock.

3.3. Mineralogy

The major mineral assemblages *via* bulk XRD experiments are identified as quartz, feldspar, carbonates, and phyllosilicate minerals such as illite, kaolinite, and chlorite. The bulk XRD analysis showed no significant mineralogical variations across the fault zone.

Clay minerals of <2 μm from the samples are illite, smectite, chlorite, and kaolinite, and were estimated by the semi-quantitative XRD method (Biscaye, 1965). The average relative percentage of illite and illite-smectite interstratifications for all the samples are ~40% and 10%, respectively, but they decrease to 25% and 7% in the gouge of the fault core. The relative percentages of chlorite and kaolinite for all samples vary between 12–16% and 32–43%, respectively, but chlorite diminishes to zero and kaolinite increases to 63–72% in the fault gouge.

The semi-quantitative results on clay minerals from XRD analysis show significant anomalies in the fault core with regards to the undisturbed and damage zone. The decrease in chlorite, illite, and illite-smectite interstratifications and the increase in kaolinite for the black-gouge zone of the fault core suggest a high degree of fluid-rock interaction and probably attest that palaeofluid channels were created within or directly adjacent to the fault core (Rossetti *et al.,* 2010).

3.4. Hydraulic pulse-tests

The fault zone permeability structure was determined through a series of hydraulic pulse-tests. The nSIGHTS (n-dimensional Statistical Inverse Graphical Hydraulic Test Simulator) code (Nuclear Waste Management Program, 2006) was used for analyzing formation pressure responses in order to identify whether the hydraulic properties of the fractured clay materials differ statistically from that of the undamaged formation (Figure 6). Preliminary pulse-tests performed in the fault zone indicated hydraulic conductivities of $5 \cdot 10^{-12}$ m s^{-1} in the fault core and overlapping damaged zone and 10^{-14} m s^{-1} in the adjacent undisturbed shale. These results were consistent with those derived from petrophysical, structural, and mineralogical data. Diagnostic plots revealed that the late-time pressure derivatives never stabilized to a constant value in the tested intervals, however, suggesting that no stable flow dimension was reached during these tests. The volume of fractured rock tested through different pulses in the same interval tended to exhibit heterogeneity that could not be represented by a single flow dimension. Thus, on the basis of the current experiments, calculation of exact hydraulic conductivities was not possible. As shown by many authors (*e.g.* Bourdet, 2002; Beauheim *et al.,* 2004; Renard *et al.,* 2008), no unique hydraulic properties can be inferred analytically in that case.

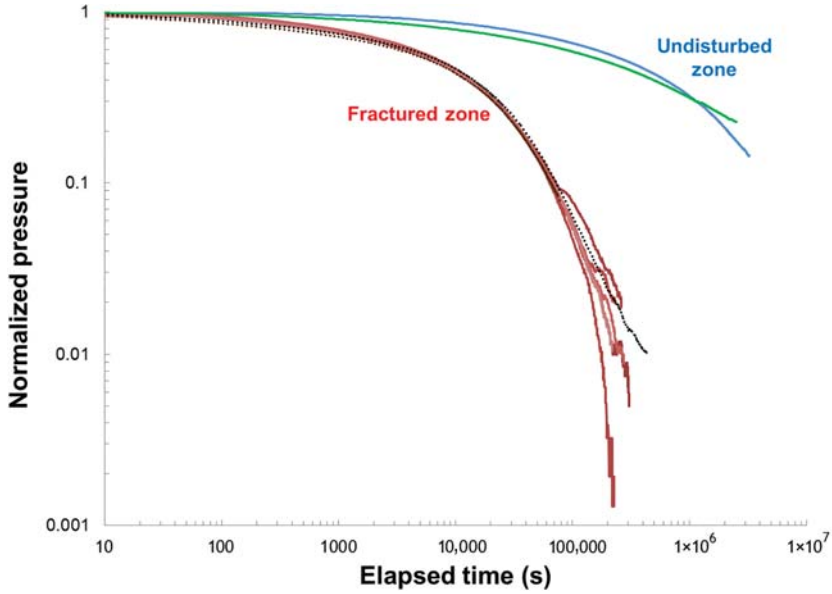

Figure 6. Normalized pulse-test data in the fractured (shades of red) and undisturbed (blue or green) zones.

4. Summary and conclusions

The Tournemire URL gives access to an unaltered polyphased strike-slip fault zone in a relatively homogeneous shale formation. The fault zone architecture consists of a heterogeneous and anastomosing fault core bounded on either side by an asymmetric damaged zone. On the one hand, the damage zone shows (1) more permeable structures consisting of a high density of macro to micro-fractures (sealed with calcite or lined with a μm-thick layer of oriented clay particles) and (2) increasing bulk porosity values toward the fault core/damage zone boundary. On the other hand, the heterogeneous distribution in the fault core of cemented cataclasites, undisturbed to moderately cleaved rocks as well as fault gouges tend to indicate a general low bulk hydraulic conductivity behavior. The numerical analyses of the pulse tests performed *in situ* within the fault zone indicate that hydraulic conductivity values are between one to two orders of magnitude greater than in the undisturbed rock. The pulse injection tests also reveal that the present testing equipment may not be suitable for estimating precisely the hydraulic properties of such structures, however, as pulse tests on fault zones are prone to induce deformation along fractures and, thus, lead to erroneous permeability and storativity values (Rutqvist, 1996; Cappa *et al.,* 2006). Nevertheless, these results indicate that fluid flow within a moderately sheared shale formation is increased along the core-damage zone boundary and such small-scale faults cannot be overlooked in terms of the long-term safety of a geological repository.

Acknowledgments

The authors are grateful to Pierre Henry, Mélody Lefèvre, Yves Gugliemi, and Christophe Nussbaum for constructive discussions and fruitful collaboration. This work is a contribution to the FRACTEX project launched by the French Institute for Radiological Protection and Nuclear Safety to assess fluid flow through natural fractures in shale formations.

Guest editor: Reiner Dohrmann

The authors and editors are grateful to anonymous reviewers who offered very helpful input and suggestions. A list of all reviewers is given at the end of the Preface for this volume.

References

Altinier, M.V., Savoye, S., Michelot, J.-L., Beaucaire, C., Massault, M., Tessier, D., and Waber, H.N. (2007) The isotopic composition of argillaceous-rocks pore water: an intercomparison study on the Tournemire argillite (France). *Physics and Chemistry of the Earth*, **32**, 209–218.

Barrett, E.P., Joyner, L.G., and Hallenda, P.P. (1951) The determination of pore volume and area distribution in porous substances: I. Computation from nitrogen isotherms. *Journal of the American Chemical Society*, **73**, 373–380.

Beauheim, R.L., Roberts, R.M., and Avis, J.D. (2004) Well testing in fractured media: Flow dimensions and diagnostic plots. *Journal of Hydraulic Research,* **42**, 69–76.

Bensenouci, F., Michelot, J.-L., Matray, J.-M., Savoye, S., Lavielle, B., and Thomas, B. (2011) A profile of Helium-4 concentration in pore-water for assessing the transport phenomena through an argillaceous formation at Tournemire (France). *Physics and Chemistry of the Earth*, **36**, 1521–1530.

Biscaye, P.E. (1965) Mineralogy and sedimentation of Recent deep-sea clay in the Atlantic Ocean and adjacent seas and oceans. *Geological Society of America Bulletin*, **76**, 803–831.

Bourdet, D. (2002) Well test analysis: the use of advanced interpretation models, Volume 3, *Handbook of Petroleum Exploration & Production*. Elsevier, Amsterdam, 426 pp.

Bretaudeau, F., Gélis, C., Leparoux, D., Brossier, R., Cabrera, J., and Côte, P. (2014) High-resolution quantitative seismic imaging of a strike fault with small vertical offset in clay rocks from underground galleries: experimental platform of Tournemire, France. *Geophysics*, **79**, B1–B18.

Brunauer, S., Emmet, P.H., and Teller, E. (1938) Adsorption of gases in multimolecular layers. *Journal of the American Chemical Society*, **60**, 309–319.

Cabrera, J. (2002) Evaluation of the 3D seismic high-resolution method at argillaceous Tournemire IRSN site. EUROSAFE2002, Berlin.

Caine, J.S., Evans, J.P., and Forster, C.B. (1996) Fault zone architecture and permeability structure. *Geology*, **24**, 1025–1028.

Cappa, F., Guglielmi, Y., Rutqvist, J., Tsang, C.-F., and Thoraval, A. (2006) Hydromechanical modelling of pulse tests that measure fluid pressure and fracture normal displacement at the Coaraze Laboratory site, France. *International Journal of Rock Mechanics & Mining Sciences*, **43**, 1062–1082.

Constantin, J., Peyaud, J.P., Vergely, P., Pagel, M., and Cabrera, J. (2004) Evolution of the structural fault permeability in argillaceous rocks in a polyphased tectonic context. *Physics and Chemistry of the Earth*, **29**, 25–41.

Cox, S.F. (1999) Deformational controls on the dynamics of fluid flow in mesothermal gold systems. Pp. 123–140 in: *Fractures, Fluid Flow and Mineralisation* (K. McCaffrey, L. Lonergan, and J.J. Wilkinson, editors). Special Publications, **155**, Geological Society, London.

Dick, P., Du Peloux de Saint Romain, A., Moreno, E., Homberg, C., Renel, F., Dauzères, A., Wittebroodt, C., and Matray, J. (2013) Structural and Petrophysical Characterization of Fault Zones in Shales: Example

from the Tournemire Url (sw, France). American Geophysical Union, Fall Meeting 2013, abstract #GP41C-1138.

Evans, J.P., Forster, C.B., and Goddard, J.V. (1997) Permeability of fault related rocks, and implications for hydraulic structure of fault zones. *Journal of Structural Geology*, **19**, 1393–1404.

Faulkner, D.R., Jackson, C.A.L., Lunn, R.J., Schlische, R.W., Shipton, Z.K., Wibberley, C.A.J., and Withjack, M.O. (2010) A review of recent developments concerning the structure, mechanics and fluid flow properties of fault zones. *Journal of Structural Geology*, **32**, 1557–1575.

Lalieux, P. and Horseman, S.T. (1996) Fluid flow through faults and fractures in argillaceous media. *Proceedings of a joint NEA/EC Workshop*, held in Berne, Switzerland, 10–12 June 1996. IBSN 92-64-16021-3. Nuclear Energy Agency, Issy-les-Moulineux, France.

Lefevre, M., Guglielmi, Y., Henry, P., Dick, P., and Gout, C. (2014) Circulation of fluids in an activated shale fault and its consequences on hydromechanical properties. 24th Réunion des Sciences de la Terre (RST), abstract #6.3.4-298.

Lefevre, M., Guglielmi, Y., Henry, P., Dick, P., and Gout, C. (2016) Calcite veins as an indicator of fracture dilatancy and connectivity during strike-slip faulting in Toarcian shale (Tournemire tunnel, Southern France). *Journal of Structural Geology*, **83**, 73–84.

Matray, J.-M., Savoye, S., and Cabrera, J. (2007) Desaturation and structure relationships around drifts excavated in the well-compacted Tournemire's argillite (Aveyron, France). *Engineering Geology*, **90**, 1–16.

Nuclear Waste Management Program (2006) *nSIGHTS* 2.40: User Manual Version 2.1. ERMS#530161. Sandia National Laboratories, Carlsbad, New Mexico, USA.

Peyaud, J.B., Pagel, M., Cabrera, J., and Pitsch, H. (2006) Mineralogical, chemical and isotopic perturbations induced in shale by fluid circulation in a fault at the Tournemire experimental site (Aveyron, France). *Journal of Geochemical Exploration*, **90**, 9–23.

Renard, P., Glenz, D., and Mejias, M. (2008) Understanding diagnostic plots for well-test interpretation. *Hydrogeology Journal*, **17**, 589–600.

Rossetti, F., Aldega, L., Tecce, F., Balsamo, F., Billi, A., and Brilli, M. (2010) Fluid flow within the damage zone of the Bocchegiano extensional fault (Larderello-Travale geothermal field, central Italy): structures, alteration and implications for hydrothermal mineralization in extensional settings. *Geological Magazine*, **148**, 558–579.

Rutqvist, J. (1996) Hydraulic pulse testing of single fractures in porous and deformable hard rocks. *Quarterly Journal of Engineering Geology*, **29**, 181–192.

Sammaljärvi, J., Jokelainen, L., Ikonen, J., and Siitari-Kauppi, M., (2012) Free radical polymerisation of MMA in brick and Grimsel Granodiorite. *Engineering Geology*, **135–136**, 52–59.

Savoye, S., de Windt, L., Beaucaire, C., Bruno, G., and Guitard, N. (2001) Are artificial tracers conservative in argillaceous media? The Tournemire claystone case. *Water Rock Interaction*, **10**, 1383–1386.

Savoye, S., Cabrera, J., and Matray, J.-M. (2003) Different hydraulic properties of single fracture in argillaceous medium: the case of the IRSN Tournemire site (France). Pp. 383–384 in: *Groundwaters in Fractured Rocks* (J. Krásný, Z. Hrkal, and J. Bruthans, editors). International Hydrological Program-VI, series on groundwater, No. **7**.

Seebeck, H., Nicol, A., Walsh, J.J., Childs, C., Beetham, R.D., and Pettinga, J. (2014) Fluid flow in fault zones from an active rift. *Journal of Structural Geology*, **62**, 52–64.

Wibberley, C.A.J., Yeilding, G., and Di Toro, G. (2008) Recent advances in the understanding of fault internal structure: a review. Pp. 5–33 in: *The Internal Structure of Fault Zones: Implications for Mechanical and Fluid Flow Properties* (C.A.J. Wibberley *et al.,* editors). Special Publications, **299**, Geological Society, London.